ACS APPLIED MATERIALS & INTERFACES

Research Article

Cite This: ACS Appl. Mater. Interfaces XXXX, XXX, XXX−XXX

www.acsami.org

Thermal-Responsive Photonic Crystal with Function of Color Switch Based on Thermochromic System

Fangfang Liu,[†] Shufen Zhang,[†] Xin Jin,[‡] Wentao Wang,[§] and Bingtao Tang*[,†,‡]

[†]State Key Laboratory of Fine Chemicals, Dalian University of Technology, Dalian 116024, China

[‡]Eco-chemical Engineering Cooperative Innovation Center of Shandong, Qingdao University of Science and Technology, Qingdao 266042, China

[§]Key Laboratory of Advanced Textile Materials and Manufacturing Technology, Ministry of Education, Zhejiang Sci-Tech University, Hangzhou 310018, China

Supporting Information

ABSTRACT: Responsive photonic crystals have attracted considerable attention. The responsiveness is usually achieved through the variation of reflection wavelengths based on Bragg diffraction. However, distinguishing external stimuli from intrinsic angle dependence is a challenge. Herein, a novel thermal-responsive photonic crystal was constructed based on the synergistic effect of the low-angle dependence of SnO_2 inverse opals and a thermochromic phase change system. The organic thermochromic phase change system was obtained by mixing the fluoran dye (heat-sensitive red TF-R_2), bisphenol A, and aliphatic alcohols in a certain proportion. By filling the thermochromic phase change system into SnO_2 inverse opals, the thermal-responsive photonic crystal was fabricated. Through simple external thermal stimulation, the mutual transformation of low-angle-dependent structural color and pigmentary color is realized and inverse opal patterns can be displayed and hidden. The proposed system, while preventing the interference of the observation angle to the thermal stimulation, shows potential application prospect in the fields of anti-counterfeiting and information encryption fields.

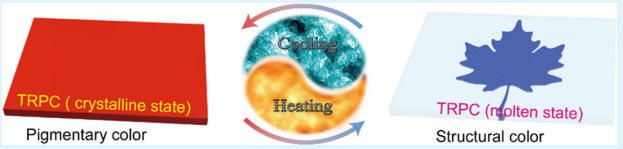

KEYWORDS: *thermal response, photonic crystal, fluoran dyes, thermochromic phase change system, color switch*

INTRODUCTION

The photonic crystal, which can generate a band gap, is a kind of highly ordered structure containing materials with different dielectric constants.[1−5] The structural colors are produced when the band gap is located in the visible region.[6−9] The color generation mechanism of photonic crystals follows Bragg's law ($\lambda = 2d\sqrt{{n_{\text{eff}}}^2 - \sin^2\alpha}$), and the reflection peaks (λ) directly relate to the refractive index (n_{eff}), the periodic lattice constant (d), and observation angle (α).[10−12] Extensive research on responsive photonic crystals based on Bragg's law has been carried out.[13−16]

Responsive photonic crystals' properties can be adjusted by external stimuli.[17−24] They play important roles in color displays, biological and chemical sensors, and many optically sensitive devices.[25−27] Generally, the responsiveness of photonic crystals is realized through the variation of reflection wavelengths resulting from changes in refractive indexes and periodic lattice constants based on Bragg diffraction.[28−30] For example, Couturier et al. fabricated dual-responsive inverse opal hydrogels, whose response to analytes can be detected through changes in optical signals based on changes in periodic lattice constants.[31] Quan et al. introduced an inverse opal structure into a shape-memory polymer material and realized the color switching by the shrink/swell effect of the polymer chain triggered by external stimuli, such as thermal stimuli.[32] However, the responsiveness is inevitably affected by observation angles due to Bragg diffraction.[33] Therefore, designing a stimulus-driven color-switching system of structural colors with minimum dependence on observation angles is a great challenge.

In this work, a novel thermal-responsive photonic crystal (TRPC) was developed by combining the SnO_2 inverse opals and thermochromic phase change system (TC-PCS) (Figure 1). In addition to the intrinsic light scattering of SnO_2 inverse opals, the increased effective refractive index[34,35] induced by incorporating TC-PCS into their pores also leads to the low-angle dependence of TRPC. TC-PCS was used to achieve a color switch through the temperature modulation of the

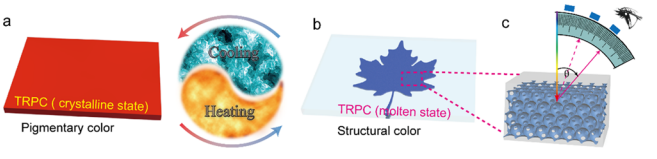

Figure 1. Schematic of the thermal response of the chromogenic material consists of SnO_2 inverse opal and thermochromic phase change system. (a) TRPC in crystalline state, (b) TRPC in molten state, and (c) detail enlargement of the patterned part, which shows low-angle dependence.

Received: September 10, 2019
Accepted: September 23, 2019
Published: September 23, 2019

Downloaded via NEWCASTLE UNIV on October 21, 2019 at 16:34:03 (UTC).
See https://pubs.acs.org/sharingguidelines for options on how to legitimately share published articles.

© XXXX American Chemical Society

DOI: 10.1021/acsami.9b16411
ACS Appl. Mater. Interfaces XXXX, XXX, XXX−XXX

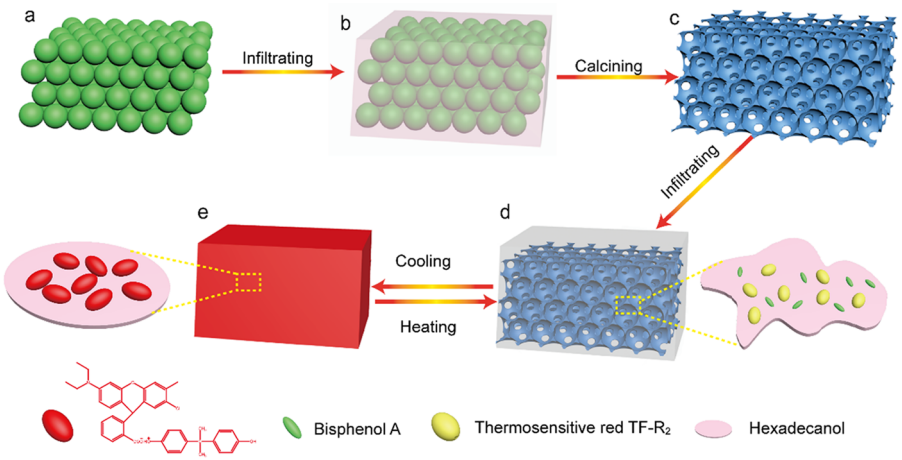

Figure 2. Schematic of the process of the fabrication of the novel thermal-responsive photonic crystal (TRPC). (a) PS template, (b) PS template infiltrating the SnO_2 precursor, (c) SnO_2 inverse opal, (d) TRPC in molten state, and (e) TRPC in crystalline state.

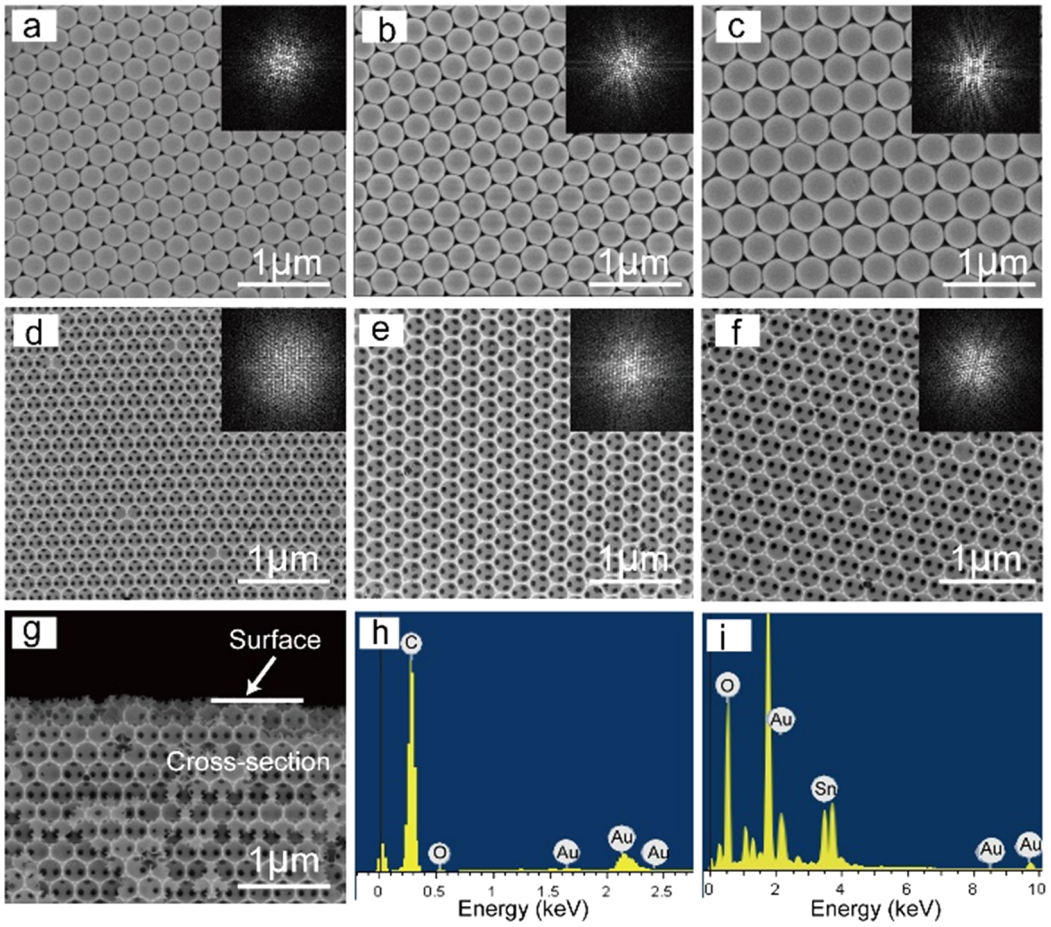

Figure 3. SEM images of PS templates and SnO_2 inverse opals. (a)−(c) PS templates with diameters of 251, 305, and 368 nm. (d)−(f) SnO_2 inverse opals with pore sizes of 168, 218, and 242 nm. FFT power spectra of SEM images are inserted at the top right-hand corner of each figure. (g) SEM image of the SnO_2 inverse opal cross section. (h) EDS spectra of PS template. (i) EDS spectra of SnO_2 inverse opal.

thermosensitive dye, bisphenol A (BPA), and phase change material (PCM). When the temperature was lower than the phase transition temperature, the pigmentary color was observed and the structural color remained hidden (Figure 1a). After the temperature reached the phase transition temperature, the pigmentary color of the TC-PCS disappeared and the structural color with low-angle dependence appeared, which effectively distinguishes the color changes caused by external stimuli (Figure 1b,c). On the basis of this transformation, inverse opal patterns can be visually displayed and hidden for potential applications in anti-counterfeiting and information encryption fields.

EXPERIMENTS AND METHODS

Materials. Polystyrene spheres were prepared by emulsion polymerization. $SnCl_4 \cdot 5H_2O$ was purchased from Xilong Scientific. A

DOI: 10.1021/acsami.9b16411
ACS Appl. Mater. Interfaces XXXX, XXX, XXX−XXX

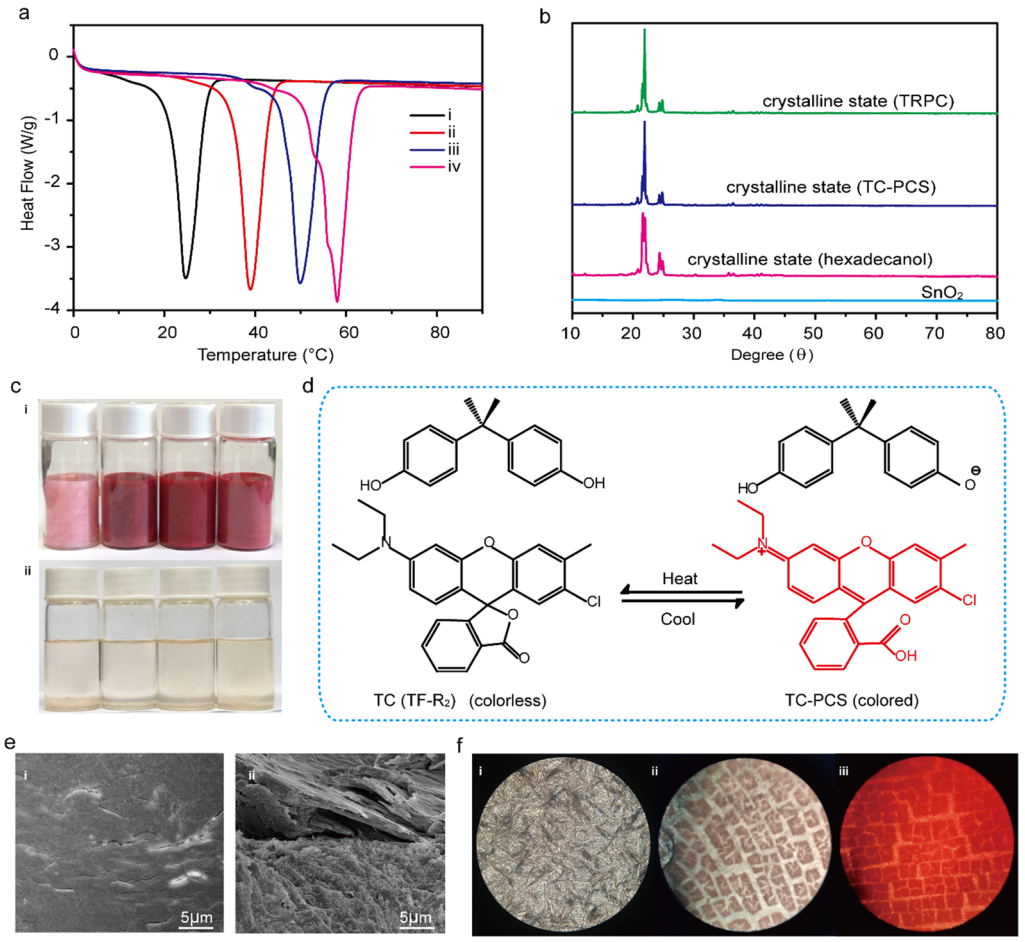

Figure 4. (a) DSC curves of the TC-PCS. (b) XRD patterns of hexadecanol, TC-PCS, and TRPC in crystalline states. (c) Optical photograph of the TC-PCSs obtained at different temperatures: (i) 20 °C (room temperature) and (ii) 70 °C. The four samples, corresponding to different phase change materials, are lauryl alcohol, tetradecanol, hexadecanol, octadecanol, respectively. (d) Schematic of the color change process of the TC-PCS. (e) SEM images of TRPC: (i) surface and (ii) cross section. (f) Polarizing optical microscope photos (×100): (i) hexadecanol, (ii) TRPC in the molten state, and (iii) TRPC in the crystalline state.

Dow Corning SYLGARD 184 silicone elastomer kit was purchased to make the mask. Bisphenol A, lauryl alcohol, tetradecanol, hexadecanol, and octadecanol were all obtained from Damao Chemical Reagent Factory. Heat-sensitive red TF-R_2 was bought from Wuhan lullaby pharmaceutical chemical Co., Ltd.

Fabrication of the Patterned SnO_2 Inverse Opal. Polystyrene (PS) microspheres with diameters of 251, 305, and 368 nm measured by SEM, whose standard deviation were 5.7, 3.2, and 5.5 respectively, were used as templates. A silicon elastomer and a curing agent were used at a mass ratio of 10:1, and after curing at 80 °C, they were cut into a maple pattern. The mask was adhered to the glass slide, and 100 μL of PS emulsion was spread out in the pattern. After the thermally assisted assembly process, the mask was removed. The precursor, which was prepared from $SnCl_4{\cdot}5H_2O$ and ethanol, was filled into the voids of the PS templates at a volume ratio of 3:5. Afterward, they were calcined in a muffle furnace in air to obtain the inverse opal structures. During calcination, the temperature raised to 500 °C at a speed of 2 °C/min and then kept for 3 h. For the fabrication of a two-dimensional code, 300 μL of PS emulsion was directly spread on the glass substrate (25 × 38 cm), the other procedures were the same as the maple pattern.

Fabrication of the Thermal-Responsive Photonic Crystal. The thermochromic (TC, heat-sensitive red TF-R_2) was mixed with BPA and PCM in the molten state at a mass ratio of 1:2:100 at 90 °C. After fully dissolving, the mixture was cooled to room temperature and the TC-PCS was obtained. The TC-PCS was dissolved in ethanol at a 1:1 volume ratio, and 300 μL of the solution was filled into the SnO_2 inverse opal. With the evaporation of ethanol, TRPC was obtained.

Characterization. The morphologies of the PS opals and SnO_2 inverse opals were analyzed using a Nova Nano SEM 450 scanning electron microscope after being coated with a layer of Au. The powder X-ray diffraction patterns were obtained with a Rigaku SmartLab X-ray diffractometer. Data were collected via Cu Kα radiation (λ = 1.5405 Å) scanning from 10° to 80° (2θ) at a rate of 20°/min. The phase transition points of the TC-PCS were obtained via differential scanning calorimetry (DSC) using a 910S system (TA Instruments, USA). The reflectance spectra were characterized using a fiber optical spectrometer (EQ 2000).

RESULTS AND DISCUSSION

Preparation of the Thermal-Responsive Photonic Crystal. The preparation of SnO_2 inverse opals was an important part of the production of the novel TRPC. A direct template method was applied to the fabrication of inverse opals (Figure 2). The PS emulsion was dropped on the glass substrate, which was placed on a hot plate. After the self-assembly, the PS spheres were arranged into a closely packed face-centered cubic (fcc) arrangement (Figure 2a), and the SnO_2 precursor prepared from $SnCl_4{\cdot}5H_2O$ and ethanol was infiltrated into the voids (Figure 2b). After calcination, the template was removed and patterned SnO_2 inverse opals were obtained (Figure 2c). The TC-PCS was then filled into the pores of the SnO_2 inverse opals to obtain the novel TRPC (Figure 2d,e). On the basis of the

DOI: 10.1021/acsami.9b16411
ACS Appl. Mater. Interfaces XXXX, XXX, XXX−XXX

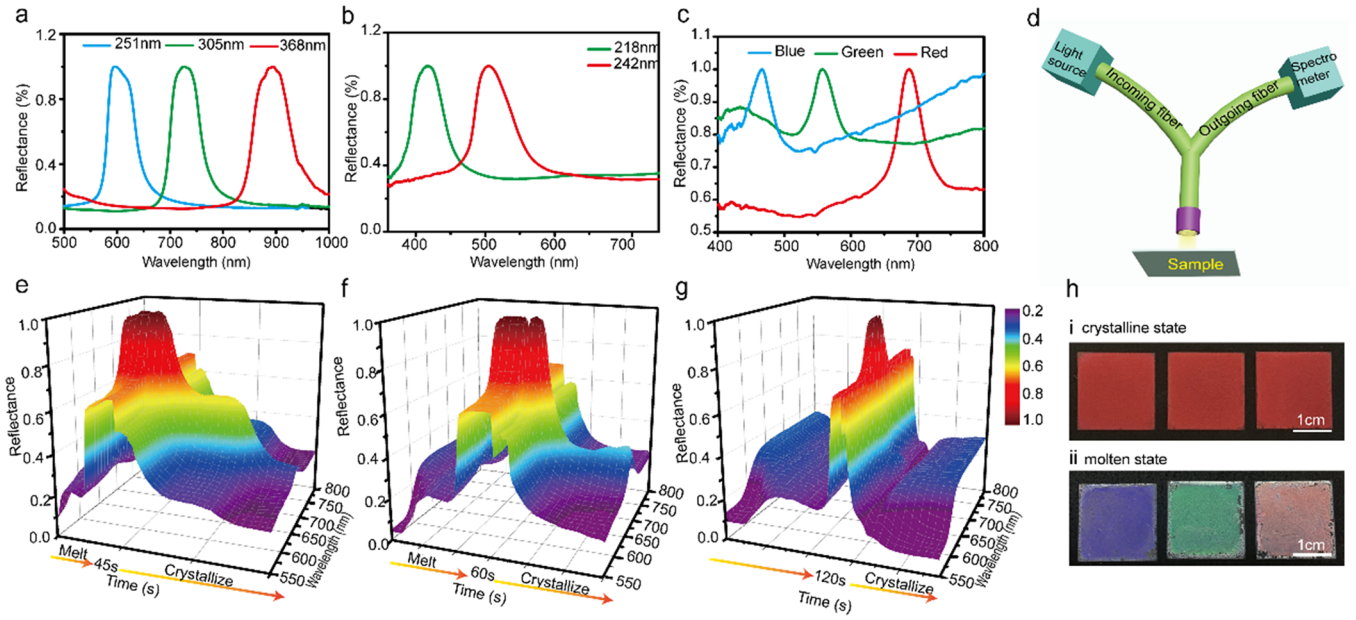

Figure 5. Reflection spectra of corresponding samples tested by the fiber optical spectrometer. The data were processed by normalization. (a) PS opals, (b) SnO_2 inverse opals, and (c) TRPCs in molten state. The lines of corresponding samples are in the same color. (d) Description of the test by optical fiber spectrometer. (e)−(g) Dynamic monitoring reflection spectra of the transformation of pigmentary color and structural color of TRPC. They are corresponding to different phase change materials tetradecanol, hexadecanol, and octadecanol, respectively. The data were processed by normalization. (h) Optical photographs of the TRPCs taken in different states.

thermal-driven phase transfer, the TRPC achieved a thermal response through the interconversion of the structural and pigmentary colors.

By changing the emulsifier amount used in the emulsion polymerization,[36] PS spheres with three sizes (251, 305, and 368 nm measured by SEM), regular morphology, and uniform particle sizes were first fabricated (Figure S1) and the measured zeta potential of the three PS spheres are −28.2, −31.3, and −30.6 mV (Table S1). The large zeta potentials enable a strong electrostatic repulsion force between PS spheres, beneficial for both excellent stability of PS emulsion and self-assembly of PS spheres into fcc arrays. Through thermally assisted self-assembly, the spheres were arranged into fcc arrays (Figure 3a−c). Given the good fluidity of SnO_2 precursors, the template array was hardly destroyed during the infiltration process and the fcc arrangement of the PS spheres was maintained (Figure S2). Meanwhile, the structure of the SnO_2 inverse opals was obtained and retained in the same array (Figure 3d−f), and the pore sizes of inverse opals were 168, 218, and 242 nm. The 2D fast Fourier-transform spectra shown in the upper right corner of Figure 3a−f further verified that the SnO_2 inverse opals retained the same fcc arrangement as PS opal templates. The SEM images of the SnO_2 inverse opal cross section (Figure 3g) also exhibited a good fcc arrangement. The thicknesses of the PS templates and SnO_2 inverse opals were 48 and 28 μm, respectively (Figure S3a−b). The EDS spectra of the PS templates and SnO_2 inverse opals (Figure 3h-i) proved that the inverse opal samples obtained after calcination were indeed composed of tin and oxygen.

The TC (TF-R_2) displays the thermochromic phenomenon under the combined effect of the chromogenic agent and the solvent. Thus, the heat-sensitive red TF-R_2 was mixed with BPA and dissolved in PCM (lauryl alcohol, tetradecanol, hexadecanol, or octadecanol) to obtain TC-PCS. The phase transition temperatures for the TC-PCS were 24.7, 38.9, 49.9, and 58.1 °C (Figure 4a), corresponding to lauryl alcohol, tetradecanol, hexadecanol, and octadecanol as solvents, respectively. Obviously, the stimulus temperature of the TC-PCS was controlled by the solvent. Also, the TC-PCS has almost the same characteristic diffraction peak as hexadecanol as shown in Figure 4b. Corresponding to the phase transition temperatures, the optical photos were also obtained at different temperatures (Figure 4c and Figure S4). At room temperature (20 °C), the TC-PCS was in the crystallization state and presented a rich red pigmentary color (Figure 4c-i). That is because the red TF-R_2 opened the lactone ring and formed a quinone structure, which was in color states (Figure 4d). When the temperature was higher than the phase transition temperature and the TC-PCS was in a molten state, the red pigmentary color became colorless and transparent (Figure 4c-ii and Figure S4). By this time, the lactone of TC (TF-R_2) was in a closed loop and in a leuco state (Figure 4d).[37,38] Here, the phase change materials were used as organic solvents and acted as a medium in which the TC (TF-R_2) reacted with bisphenol A based on the electron transfer. Meanwhile, its phase transition temperature determined the response temperature.[39,40]

TRPC was obtained after the TC-PCS was filled into the pores of the SnO_2 inverse opals. The SEM images of the surface and the cross section of the TRPC (Figure 4e) indicated that the TC-PCS completely filled the pores and covered the surface of the inverse opals and the thickness of TRPC was 91 μm (Figure S3c). The XRD patterns of TRPC were evidently the same as that of TC-PCS and the solvent (Figure 4b) and showed the same crystallization morphology as recorded with a polarizing microscope (Figure 4f-i,ii). When the TRPC was in a molten state, the crystal of TC-PCS completely disappeared (Figure 4f-ii). When the TRPC was in a crystallization state, the crystal form (Figure 4f-iii) was the same as that of the solvent (Figure 4f-i). Given the color rendering, the polarizing optical microscope photos presented a fine red color (Figure 4f-iii).[41] Meanwhile, the crystallization process of the solvent and TRPC was also recorded, as shown in Movies S1 and S2.

DOI: 10.1021/acsami.9b16411
ACS Appl. Mater. Interfaces XXXX, XXX, XXX−XXX

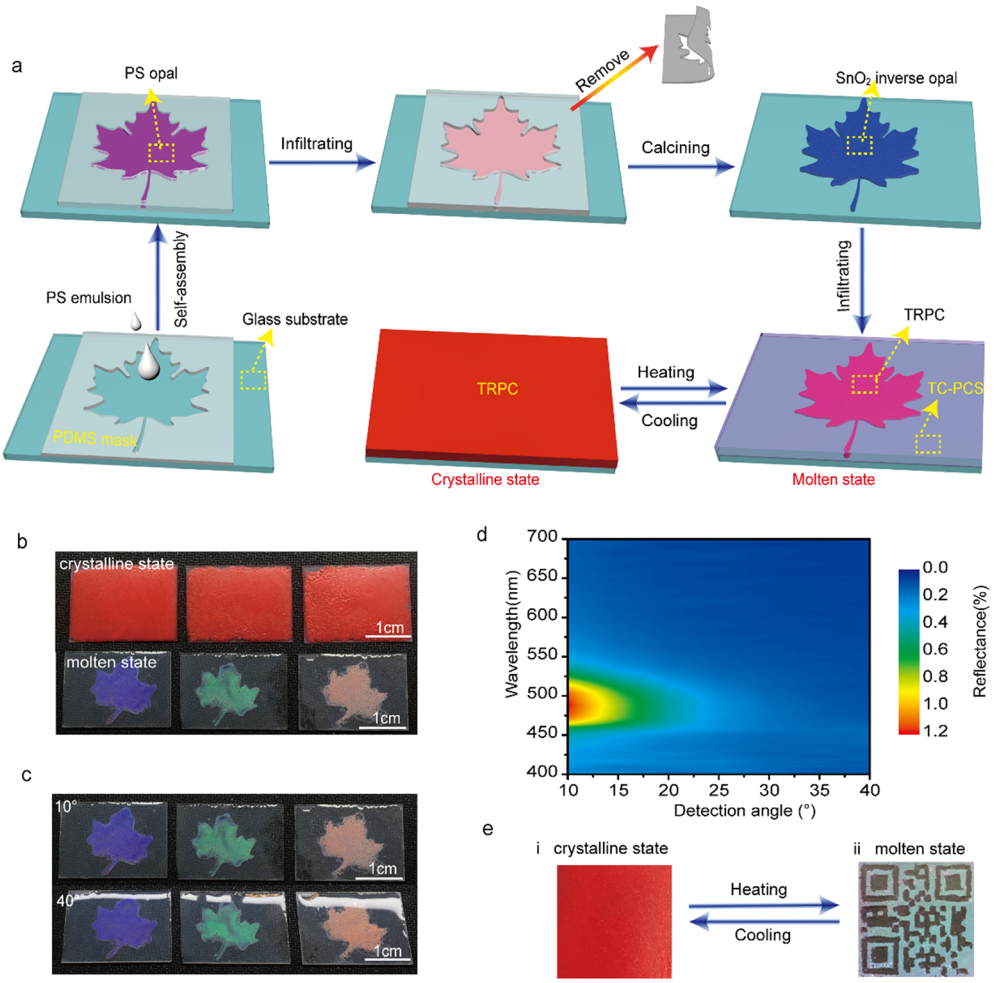

Figure 6. (a) Schematic of the process of the fabrication of the bio-inspired composite color-changing material (TRPC). (b) Optical photographs of the TRPCs taken in different states. (i) The TRPCs were in the molten state, and (ii) the TRPCs were in the crystalline state at room temperature. (c) Optical photographs of the TRPCs in the molten state with the shooting angles of 10° and 40°. (d) Diffuse scattering spectra of inverse opal (the pores size is 242 nm) films under the detection angles ranging from 10° to 40° with the incident angle fixed at 0°. (e) The optical photos of hidden and reproduced of the two-dimensional code "DUT".

Optical Property of the Thermal-Responsive Photonic Crystal. The reflection spectra of the PS templates, SnO_2 inverse opals, and TRPC in a molten state were all measured using a fiber optical spectrometer (Figure 5a–c). The Y-type optical fiber was used for the detection, whose light source was perpendicular to the sample (Figure 5d). The wavelength peak positions of the PS opals with 251, 305, and 368 nm were 602, 727, and 892 nm (Figure 5a), respectively. The corresponding peak positions of the other SnO_2 inverse opals with pore sizes of 218 and 242 nm were 415 and 504 nm (Figure 5b), respectively. The peak positions of reflection spectra of the TRPC in a molten state were 466, 558, and 687 nm corresponding to blue, green, and red colors, respectively (Figure 5c). Because of the difference in the refractive index between TC-PCS and SnO_2, the characteristics of the photonic crystal still exist and the structural color will present when TC-PCS is in the molten state.

Given that the TC-PCS showed different color states, the thermal response was achieved by the conversion between the pigmentary color and structural color under thermal drives. The conversion processes were dynamically monitored using a fiber optical spectrometer under heating (72 °C) and natural cooling conditions. The transformation process of the TRPC with tetradecanol, hexadecanol, or octadecanol was dynamically measured, as shown in Figure 5e–g. With the absorption of heat, the spectrum changed from no reflection peak (showing the pigmentary color in crystalline state, Figure 5h-i) to a significant reflection peak and the reflectivity gradually increased until stabilized (Figure 5e–g, showing the structural color in the molten state, Figure 5h-ii). After removing the heat source, the reflection spectrum showed an opposite trend to that in the presence of the heat source and the reflection peak gradually disappeared (Figure 5e–g, after 45, 60, and 120 s, respectively). Accordingly, the structural colors disappeared and changed into pigmentary colors (Figure 5h-i).

Pattern of the Thermal-Responsive Photonic Crystal. Given that the PDMS has good affinity to glass substrates, the PDMS mask limited the PS assembly area and resulted in patterned inverse opals (Figure 6a). As shown in Figure 6b, the patterns were hidden and reproduced using the thermal response properties of the TRPC. At room temperature, that is, when the TC-PCS was in the crystallization state, the TRPC presented excellent red pigmentary colors derived from the TC-PCS. When the PCM absorbed enough heat to melt, the pigmentary colors disappeared and presented patterns with structural colors. For the structural colors displayed in a molten state (Figure 6c), the optical photographs were gotten at 10° and

DOI: 10.1021/acsami.9b16411
ACS Appl. Mater. Interfaces XXXX, XXX, XXX–XXX

40° and the colors observed were similar and exhibited low-angle dependence. As shown in Figure 6d, the diffused scattering spectra of the SnO_2 inverse opals slightly changed with the detection angle increasing from 10° to 40°. The infiltration of the TC-PCS further increased the material's effective refractive index, and thus, the low-angle dependence was maintained. Based on the low-angle dependence of structural colors, the color changes caused by external stimuli can be effectively highlighted while minimizing the dependence of the observation angle. Through simple external thermal simulation, the mutual transformation of low-angle-dependent structural color and pigmentary color is realized, and it has a potential application prospect in the thermal-driven anti-counterfeiting field.

Based on the above features, it was also applied to information encryption. The inverse opal was prepared into the pattern of a two-dimensional code. After filling with TC-PCS, the information was controlled to hidden (Figure 6e-i) and reproduced (Figure 6e-ii) by a thermal stimulus. After heating, the TC-PCS melt and transferred into a transparent state and present a two-dimensional code (Figure 6e-ii), and the information stored in two-dimensional code "DUT" can be read scanning by phone (Movie S3).

CONCLUSIONS

A novel TRPC was successfully obtained in this work. Patterned SnO_2 inverse opals were fabricated via the direct template method, and a PDMS mask was used to limit the assembly areas. The thermal sensitivity was obtained by mixing TC ($TF\text{-}R_2$) with BPA and PCM, whereas the thermosensitivity temperature was regulated by the PCM. The successful combination of structural and pigmentary colors with an effective thermal response was achieved through the conversion between pigmentary and structural colors by filling the TC-PCS into the SnO_2 inverse opals. When the temperature was lower than the phase transition temperature, that is, the crystallization state, the TRPC presented an excellent pigmentary color. When the temperature was higher than the phase transition temperature, that is, the molten state, the structural color appeared with the disappearance of the pigmentary color. Based on the synergistic effect of the low-angle-dependent SnO_2 inverse opals and TC-PCS, the low-angle dependence of structural colors can effectively highlight the color changes caused by external stimuli. Meanwhile, inverse opal patterns were also successfully displayed and hidden via a thermal response and successfully applied to the information encryption.

ASSOCIATED CONTENT

Supporting Information

The Supporting Information is available free of charge on the ACS Publications website at DOI: 10.1021/acsami.9b16411.

SEM images of PS spheres, size measurement of PS emulsion, SEM images of PS templates with SnO_2 precursor infiltrated in the voids, and optical photograph of the TC-PCSs obtained at different temperatures (PDF)

Crystallization process of hexadecanol under a polarizing optical microscope (MP4)

Crystallization process of TRPC under a polarizing optical microscope (MP4)

Display and reading process of a two-dimensional code (MOV)

AUTHOR INFORMATION

Corresponding Author

*E-mail: tangbt@dlut.edu.cn.

ORCID

Shufen Zhang: 0000-0003-3390-4199

Xin Jin: 0000-0001-8816-9705

Bingtao Tang: 0000-0001-5201-9924

Author Contributions

The manuscript was written through contributions of all authors. All authors have given approval to the final version of the manuscript.

Notes

The authors declare no competing financial interest.

ACKNOWLEDGMENTS

This work was supported by the National Natural Science Foundation of China (21878043, 21576039, 21276042, 21421005, and U1608223), the Fundamental Research Funds for the Central Universities (DUT18ZD218), Talent Fund of Shandong Collaborative Innovation Center of Eco Chemical Engineering (XTCXYX04), and Innovative Talents of Colleges and Universities in Liaoning Province (LCR2018066).

REFERENCES

(1) Joannopoulos, J. D.; Villeneuve, P. R.; Fan, S. Photonic Crystals: Putting a New Twist on Light. *Nature* **1997**, *386*, 143.

(2) Segal, N.; Keren-Zur, S.; Hendler, N.; Ellenbogen, T. Controlling Light with Metamaterial-Based Nonlinear Photonic Crystals. *Nat. Photonics* **2015**, *9*, 180.

(3) Meng, Z.-J.; Zhang, J.; Deng, X.; Liu, J.; Yu, Z.; Abell, C. Bioinspired Hydrogel Microfibres Colour-Encoded with Colloidal Crystals. *Mater. Horiz.* **2019**, DOI: 10.1039/c9mh00528e.

(4) Lee, G. H.; Kim, J. B.; Choi, T. M.; Lee, J. M.; Kim, S.-H. Structural Coloration with Nonclose-Packed Array of Bidisperse Colloidal Particles. *Small* **2019**, *15*, 1804548.

(5) Lee, C. H.; Yu, J.; Wang, Y.; Tang, A. Y. L.; Kan, C. W.; Xin, J. H. Effect of Graphene Oxide Inclusion on the Optical Reflection of a Silica Photonic Crystal Film. *RSC Adv.* **2018**, *8*, 16593.

(6) Li, F.; Tang, B.; Wu, S.; Zhang, S. Facile Synthesis of Monodispersed Polysulfide Spheres for Building Structural Colors with High Color Visibility and Broad Viewing Angle. *Small* **2017**, *13*, 1602565.

(7) Wang, F.; Zhang, X.; Lin, Y.; Wang, L.; Zhu, J. Structural Coloration Pigments Based on Carbon Modified $ZnS@SiO_2$ Nanospheres with Low-Angle Dependence, High Color Saturation, and Enhanced Stability. *ACS Appl. Mater. Interfaces* **2016**, *8*, 5009.

(8) Yang, X.; Ge, D.; Wu, G.; Liao, Z.; Yang, S. Production of Structural Colors with High Contrast and Wide Viewing Angles from Assemblies of Polypyrrole Black Coated Polystyrene Nanoparticles. *ACS Appl. Mater. Interfaces* **2016**, *8*, 16289.

(9) Zhang, J.; Zhu, Z.; Yu, Z.; Ling, L.; Wang, C.-F.; Chen, S. Large-Scale Colloidal Films with Robust Structural Colors. *Mater. Horiz.* **2019**, *6*, 90.

(10) Sano, K.; Kim, Y. S.; Ishida, Y.; Ebina, Y.; Sasaki, T.; Hikima, T.; Aida, T. Photonic Water Dynamically Responsive to External Stimuli. *Nat. Commun.* **2016**, *7*, 12559.

(11) Jiang, Y.; Xu, D.; Li, X.; Lin, C.; Li, W.; An, Q.; Tao, C.-a.; Tang, H.; Li, G. Electrothermally Driven Structural Colour Based on Liquid Crystal Elastomers. *J. Mater. Chem.* **2012**, *22*, 11943.

(12) Aguirre, C. I.; Reguera, E.; Stein, A. Tunable Colors in Opals and Inverse Opal Photonic Crystals. *Adv. Funct. Mater.* **2010**, *20*, 2565.

(13) Fu, Q.; Zhu, H.; Ge, J. Electrically Tunable Liquid Photonic Crystals with Large Dielectric Contrast and Highly Saturated Structural Colors. *Adv. Funct. Mater.* **2018**, *28*, 1804628.

DOI: 10.1021/acsami.9b16411
ACS Appl. Mater. Interfaces XXXX, XXX, XXX−XXX

(14) Puzzo, D. P.; Arsenault, A. C.; Manners, I.; Ozin, G. A. Electroactive Inverse Opal: a Single Material for All Colors. *Angew. Chem., Int. Ed.* **2009**, *48*, 943.
(15) Zhou, L.; Li, Y.; Liu, G.; Fan, Q.; Shao, J. Study on the Correlations between the Structural Colors of Photonic Crystals and the Base Colors of Textile Fabric Substrates. *Dyes Pigm.* **2016**, *133*, 435.
(16) Schroden, R. C.; Al-Daous, M.; Blanford, C. F.; Stein, A. Optical Properties of Inverse Opal Photonic Crystals. *Chem. Mater.* **2002**, *14*, 3305.
(17) Diao, Y. Y.; Liu, X. Y.; Toh, G. W.; Shi, L.; Zi, J. Multiple Structural Coloring of Silk-Fibroin Photonic Crystals and Humidity-Responsive Color Sensing. *Adv. Funct. Mater.* **2013**, *23*, 5373.
(18) Ma, B.; Ju, X.-J.; Luo, F.; Liu, Y.-Q.; Wang, Y.; Liu, Z.; Wang, W.; Xie, R.; Chu, L.-Y. Facile Fabrication of Composite Membranes with Dual Thermo- and pH-Responsive Characteristics. *ACS Appl. Mater. Interfaces* **2017**, *9*, 14409.
(19) Fang, Y.; Ni, Y.; Choi, B.; Leo, S.-Y.; Gao, J.; Ge, B.; Taylor, C.; Basile, V.; Jiang, P. Chromogenic Photonic Crystals Enabled by Novel Vapor-Responsive Shape-Memory Polymers. *Adv. Mater.* **2015**, *27*, 3696.
(20) Chen, K.; Fu, Q.; Ye, S.; Ge, J. Multicolor Printing Using Electric-Field-Responsive and Photocurable Photonic Crystals. *Adv. Funct. Mater.* **2017**, *27*, 1702825.
(21) Stein, A.; Wilson, B. E.; Rudisill, S. G. Design and Functionality of Colloidal-Crystal-Templated Materials-Chemical Applications of Inverse Opals. *Chem. Soc. Rev.* **2013**, *42*, 2763.
(22) Schäfer, C. G.; Winter, T.; Heidt, S.; Dietz, C.; Ding, T.; Baumberg, J. J.; Gallei, M. Smart Polymer Inverse-Opal Photonic Crystal Films by Melt-Shear Organization for Hybrid Core−Shell Architectures. *J. Mater. Chem. C* **2015**, *3*, 2204.
(23) Schäfer, C. G.; Gallei, M.; Zahn, J. T.; Engelhardt, J.; Hellmann, G. P.; Rehahn, M. Reversible Light-, Thermo-, and Mechano-Responsive Elastomeric Polymer Opal Films. *Chem. Mater.* **2013**, *25*, 2309.
(24) Phillips, K. R.; England, G. T.; Sunny, S.; Shirman, E.; Shirman, T.; Vogel, N.; Aizenberg, J. A Colloidoscope of Colloid-Based Porous Materials and Their Uses. *Chem. Soc. Rev.* **2016**, *45*, 281.
(25) Ge, J.; Yin, Y. Responsive Photonic Crystals. *Angew. Chem., Int. Ed.* **2011**, *50*, 1492.
(26) Kelly, J. A.; Shukaliak, A. M.; Cheung, C. C. Y.; Shopsowitz, K. E.; Hamad, W. Y.; MacLachlan, M. J. Responsive Photonic Hydrogels Based on Nanocrystalline Cellulose. *Angew. Chem., Int. Ed.* **2013**, *52*, 8912.
(27) Wang, W.; Fan, X.; Li, F.; Qiu, J.; Umair, M. M.; Ren, W.; Ju, B.; Zhang, S.; Tang, B. Magnetochromic Photonic Hydrogel for an Alternating Magnetic Field-Responsive Color Display. *Adv. Opt. Mater.* **2018**, *6*, 1701093.
(28) Honda, M.; Kataoka, K.; Seki, T.; Takeoka, Y. Confined Stimuli-Responsive Polymer Gel in Inverse Opal Polymer Membrane for Colorimetric Glucose Sensor. *Langmuir* **2009**, *25*, 8349.
(29) Zhao, Y.; Xie, Z.; Gu, H.; Zhu, C.; Gu, Z. Bio-Inspired Variable Structural Color Materials. *Chem. Soc. Rev.* **2012**, *41*, 3297.
(30) Liu, J.; Zhang, Y.; Zhou, R.; Gao, L. Volatile Alcohol-Responsive Visual Sensors Based on P(HEMA-co-MA)-Infiltrated SiO2inverse Opal Photonic Crystals. *J. Mater. Chem. C* **2017**, *5*, 6071.
(31) Couturier, J.-P.; Sütterlin, M.; Laschewsky, A.; Hettrich, C.; Wischerhoff, E. Responsive Inverse Opal Hydrogels for the Sensing of Macromolecules. *Angew. Chem., Int. Ed.* **2015**, *54*, 6641.
(32) Quan, M.; Yang, B.; Wang, J.; Yu, H.; Cao, X. Simultaneous Microscopic Structure Characteristics of Shape-Memory Effects of Thermo-Responsive Poly(vinylidene fluoride-co-hexafluoropropylene) Inverse Opals. *ACS Appl. Mater. Interfaces* **2018**, *10*, 4243.
(33) Bai, L.; Mai, V. C.; Lim, Y.; Hou, S.; Möhwald, H.; Duan, H. Large-Scale Noniridescent Structural Color Printing Enabled by Infiltration-Driven Nonequilibrium Colloidal Assembly. *Adv. Mater.* **2018**, *30*, 1705667.
(34) Liu, F.; Shan, B.; Zhang, S.; Tang, B. SnO2Inverse Opal Composite Film with Low-Angle-Dependent Structural Color and Enhanced Mechanical Strength. *Langmuir* **2018**, *34*, 3918.
(35) Josephson, D. P.; Popczun, E. J.; Stein, A. Effects of Integrated Carbon as a Light Absorber on the Coloration of Photonic Crystal Based Pigments. *J. Phys. Chem. C* **2013**, *117*, 13585.
(36) Liu, F.; Xiu, J.; Tang, B.; Zhao, D.; Zhang, S. Dynamic Monitoring of Thermally Assisted Assembly of Colloidal Crystals. *J. Mater. Sci.* **2017**, *52*, 7883.
(37) Oh, W.; Angupillai, S.; Muthukumar, P.; So, H.-S.; Son, Y. Synthesis of Novel tert-Butyl Substituted Fluorans and an Investigation of Their Thermochromic Behavior. *Dyes Pigm.* **2016**, *128*, 235.
(38) Huang, K.; Yue, Y.; Jiao, X.; Liu, C.; Wang, Q.; He, S.; Zhao, L.; Zeng, X. Fluorescence Regulation of 4-Aminobenzofluoran and its Applications for Cu^{2+}-Selective Fluorescent Probe and Bioimaging. *Dyes Pigm.* **2017**, *143*, 379.
(39) Burkinshaw, S. M.; Griffiths, J.; Towns, A. D. Reversibly Thermochromic Systems Based on pH-Sensitive Functional Dyes. *J. Mater. Chem.* **1998**, *8*, 2677.
(40) MacLaren, D. C.; White, M. A. Dye−Developer Interactions in the Crystal Violet Lactone−Lauryl Gallate Binary System: Implications for Thermochromism. *J. Mater. Chem.* **2003**, *13*, 1695.
(41) Yao, K.; Meng, Q.; Bulone, V.; Zhou, Q. Flexible and Responsive Chiral Nematic Cellulose Nanocrystal/poly (ethylene glycol) Composite Films with Uniform and Tunable Structural Color. *Adv. Mater.* **2017**, *29*, 1701323.

DOI: 10.1021/acsami.9b16411
ACS Appl. Mater. Interfaces XXXX, XXX, XXX−XXX